

**Figure 6.** Calculated heat of formation [ $\Delta(\Delta H_f)$ ] for radical anions of *o*- (○, ●), *m*- (△, ▲), and *p*- $\text{ClC}_6\text{H}_4\text{CH}_2\text{Cl}$  (□, ■) relative to  $\Delta H_f$  at the same C-Cl bond distance as the corresponding neutral molecules plotted against the bond-stretching distance ( $\Delta\text{C-Cl}$ ) of the Cl- $\text{C}_6\text{H}_4$  and  $\text{CH}_2\text{-Cl}$  bonds, respectively. The MNDO<sup>45,46</sup> calculations were carried out by taking each C-Cl bond distance as an independent variable with the rest of geometrical parameters being optimized. The geometrical change of the  $\text{CH}_2\text{Cl}$  group with stretching of the  $\text{CH}_2\text{-Cl}$  bond is shown as the plot of the dihedral angle ( $\theta$ ) between the aromatic ring and the  $\text{CH}_2$  planes vs  $\Delta\text{C-Cl}$ .

*p*- $\text{CNC}_6\text{H}_4\text{Cl}^-$  as compared to  $\text{PhCl}^-$  (Figure 5) agrees with the reported longer lifetime of the former radical anion.<sup>9b</sup>

The more enhanced selectivities are observed in the  $\text{AcrH}_2/\text{AcrH}^+$ -catalyzed reductive dehalogenation of halobenzylic halides

( $\text{X-C}_6\text{H}_4\text{CH}_2\text{X}$ ;  $\text{X} = \text{Cl, Br}$ ) with  $\text{NaBH}_4$  as shown in Table IV, where  $\text{X-C}_6\text{H}_4\text{CH}_3$  is obtained selectively with no detectable formation of  $\text{PhCH}_2\text{X}$  in each case. Such highly selective cleavage of the  $\text{CH}_2\text{-X}$  bond as compared to that of the  $\text{X-C}_6\text{H}_4$  bond may also indicate that the reductive dehalogenation proceeds via initial formation of the  $\pi^*$  radical anions, since the rate of reductive cleavage of the  $\text{CH}_2\text{-X}$  bond would otherwise be comparable with that of the  $\text{X-C}_6\text{H}_4$  bond, judging from the similar  $\Phi_{\infty}$  values of  $\text{PhX}$  and  $\text{PhCH}_2\text{X}$  (Table III). Figure 6 depicts the energy profiles of the reductive cleavage of both the  $\text{CH}_2\text{-Cl}$  and  $\text{Cl-C}_6\text{H}_4$  bonds calculated by a similar manner to those in Figure 5, by taking each C-Cl bond distance as an independent variable. As is clearly seen in Figure 6, the energetic barrier in the cleavage of the Cl- $\text{C}_6\text{H}_4$  bond is significantly larger than that of the  $\text{CH}_2\text{-Cl}$  bond, in agreement with the observed highly selective cleavage of the  $\text{CH}_2\text{-Cl}$  bond (Table IV). As the  $\text{CH}_2\text{-Cl}$  bond of  $\text{ClC}_6\text{H}_4\text{CH}_2\text{Cl}^-$  begins to stretch, continuous flattening of  $\text{ClC}_6\text{H}_4\text{CH}_2^-$  group occurs to yield  $\text{ClC}_6\text{H}_4\text{CH}_2^-$  and  $\text{Cl}^-$  (Figure 6).

In conclusion, the photocatalytic dehalogenation of aromatic and alkyl halides in the present system may proceed via photoinduced electron transfer from the singlet excited state of 10-methylacridine derivatives used as catalysts to the halogenated compounds, when the bond-breaking process upon the electron transfer can compete well with the back-electron-transfer process to yield the dehalogenated products efficiently. The facile reduction of the oxidized form of 10-methylacridine derivatives with  $\text{NaBH}_4$  regenerates the catalysts, constituting not only efficient but also stable photocatalytic systems.

**Acknowledgment.** This work was supported in part by a grant-in-aid (to S. Fukuzumi) for scientific research from Ministry of Education, Science and Culture, Japan. We thank Mr. Y. Tokuda for his single photon counting experiments and Mr. N. Hayashi for his involvement in the early stage of this work.

## Specific Asymmetric Fusion between Artificial and Biological Model Membranes

Tino A. A. Fonteyn,<sup>1a</sup> Dick Hoekstra,<sup>1b</sup> and Jan B. F. N. Engberts\*<sup>1a</sup>

Contribution from the Department of Organic Chemistry, University of Groningen, Nijenborgh 16, 9747 AG Groningen, The Netherlands, and Department of Physiological Chemistry, University of Groningen, Bloemsingel 10, 9712 KZ Groningen, The Netherlands. Received March 23, 1990

**Abstract:** Experimental conditions are delineated for specific asymmetric fusion, induced by  $\text{Ca}^{2+}$  ions, of vesicles formed from di-*n*-dodecyl phosphate (DDP) with phosphatidylserine (PS) and dioleoylphosphatidylcholine (DOPC) liposomes as well as with erythrocyte ghost (EG) membranes. Initial rates and extents of fusion were obtained with the resonance energy transfer assay. The merging of the bilayers rather than vesicle aggregation represents the rate-determining step in the overall fusion event. Unexpectedly, asymmetric PS-DDP and DOPC-DDP vesicle fusion does occur below the main phase-transition temperature of the DDP bilayer. At 25 °C and pH 7.4, DDP vesicles fuse with EG membranes more rapidly and efficiently than PS vesicles. The possible relevance of these findings for cell biological and drug-targetting experiments is pointed out.

Fusion of lipid bilayer membranes is a crucial biological event and occurs, for example, in processes like endo- and exocytosis, cell division, and the infectious entry of viruses into cells.<sup>2,3</sup> Because of the complexities involved in using natural cell membranes, liposomal model systems have been frequently employed to study mechanistic aspects of membrane fusion. Recently we have shown that artificial membrane vesicles formed from simple synthetic surfactants also fuse upon addition of appropriate fu-

sogenic agents and that their fusogenic activity mimics important features of phospholipid membrane fusion.<sup>4</sup> This previous work concerned the occurrence of *symmetric* vesicle fusion, i.e., merging between like vesicle bilayers. Mechanistic studies of the  $\text{Ca}^{2+}$ -

(1) (a) Department of Organic Chemistry. (b) Department of Physiological Chemistry.

(2) Ohki, S.; Doyle, D.; Flanagan, T. D.; Hui, S. W.; Mayhew, E., Eds. *Molecular Mechanisms of Membrane Fusion*; Plenum: New York, 1988.

(3) Hoekstra, D.; Kok, J. W. *Biosci. Rep.* 1989, 9, 273.

(4) (a) Rupert, L. A. M.; Hoekstra, D.; Engberts, J. B. F. N. *J. Am. Chem. Soc.* 1985, 107, 2628. (b) Rupert, L. A. M.; Engberts, J. B. F. N.; Hoekstra, D. *J. Am. Chem. Soc.* 1986, 108, 3920. (c) Rupert, L. A. M.; Van Breemen, J. F. L.; Van Bruggen, E. F. J.; Engberts, J. B. F. N.; Hoekstra, D. *J. Membr. Biol.* 1987, 95, 255. (d) Rupert, L. A. M.; Hoekstra, D.; Engberts, J. B. F. N. *J. Colloid Interface Sci.* 1987, 120, 125. (e) Rupert, L. A. M.; Van Breemen, J. F. L.; Hoekstra, D.; Engberts, J. B. F. N. *J. Phys. Chem.* 1988, 92, 4416. (f) Rupert, L. A. M.; Hoekstra, D.; Engberts, J. B. F. N. *J. Colloid Interface Sci.* 1989, 130, 271.

induced fusion of di-*n*-dodecyl phosphate (DDP) vesicles indicated that the cation forms a "cis complex" with two adjacent DDP molecules in the lateral plane of the bilayer, leading to aggregation of the vesicles. Subsequent events most likely involve the formation of an unstable inverted micellar intermediate (IMI), which is triggered by the formation of a "trans complex" between two closely apposed bilayers. Interestingly, this IMI acts as an intermediate in both the overall fusion process and a polymorphic transformation from a bilayer to a hexagonal H<sub>11</sub> packing.<sup>4c,d</sup>

In the present work, we have explored the possibilities for *asymmetric* fusion between vesicles of different chemical composition. It was found that vesicles formed from synthetic DDP<sup>5</sup> molecules can fuse with artificial phospholipid membranes (liposomes) like phosphatidylserine (PS) and dioleoylphosphatidylcholine (DOPC) vesicles as well as with biological model membranes such as erythrocyte ghosts (EG).<sup>6</sup> The results may be of direct relevance in the continuing search for fusogenic (drug) carrier systems.<sup>6</sup>

### Materials and Methods

**Materials.** Sodium di-*n*-dodecyl phosphate was prepared from di-*n*-dodecyl hydrogen phosphate (Alpha Chemicals) by adding an equimolar amount of sodium ethanolate to a solution of the acid in warm ethanol (50 °C). The surfactant was purified by crystallization. PS (bovine brain), synthetic dioleoylphosphatidylcholine (DOPC), and the fluorescent lipid analogues *N*-NBD-PE and *N*-Rh-PE were purchased from Avanti Polar Lipids, Inc. DTP was synthesized according to Bauman.<sup>7</sup> Human erythrocytes were obtained from the Red Cross Blood Bank. Erythrocyte ghosts were prepared in 5 mM sodium acetate/5 mM Hepes hemolyzing buffers (pH 7.4) according to the procedure described by Steck et al.<sup>8</sup>

**Vesicle Preparation.** DDP vesicles were prepared by the ethanol injection method.<sup>4c</sup> Here to 10 mg of DDP was dissolved in 100 μL of ethanol. This solution (80 μL) was injected into 2 mL of 5 mM sodium acetate/5 mM Hepes buffer (pH 7.4) with an Exmire microsyringe. The temperature of the buffer was kept above the main phase-transition temperature of DDP ( $T = 55$  °C;  $T_m = 29$  °C). Large unilamellar vesicles (LUV's) of PS and DOPC were prepared by reversed-phase evaporation.<sup>9</sup> The vesicles in 5 mM sodium acetate/5 mM Hepes buffers (pH 7.4) were sized by extrusion through polycarbonate Unipore membranes (Biorad; pore size 0.1 μm).

**Vesicle Aggregation.** Initial rates of aggregation were determined from continuous turbidity measurements at 400 nm (25 °C) with a Perkin-Elmer λ5 UV-vis spectrophotometer. Since aggregation is a second-order process and rates of symmetric aggregation ( $v_{agg}^{sym}$ ) can be determined separately, the rates of asymmetric aggregation ( $v_{agg}^{asym}$ ) can be obtained from  $v_{agg}^{obs} = v_{agg}^{sym} + v_{agg}^{asym}$ .

**Vesicle Fusion.** Ca<sup>2+</sup>-induced membrane fusion was followed by monitoring lipid mixing in 5 mM sodium acetate/5 mM Hepes buffers (pH 7.4) with the resonance energy transfer (RET) assay.<sup>10</sup> Vesicles labeled with 0.8 mol % each of *N*-NBD-PE and *N*-Rh-PE were mixed with an equimolar amount of unlabeled vesicles. After addition of CaCl<sub>2</sub>, the increase of *N*-NBD-PE fluorescence was followed continuously with an SLM-Aminco SPF-500 CTM spectrofluorometer equipped with a thermostated cell holder, magnetic stirring device, and a chart recorder. The excitation wavelength was 465 nm, and the emission was recorded at 530 nm. The initial fluorescence of the vesicle solution was taken as the zero level. The level of infinite dilution (100% fluorescence) was obtained after disruption of the DDP and DTP vesicles in cetyltrimethylammonium bromide (CTAB, 1% w/v) solutions and of phospholipid vesicles in Triton X-100 (1% w/v) solutions. Corrections were applied for sample dilution and effects of CTAB and Triton X-100 on the quantum yield of *N*-NBD-PE.<sup>4</sup>

Generally, the time scale of the fusion processes is reflected in the initial rates of fusion. At 25 °C, Ca<sup>2+</sup>-induced fusion activity was monitored during a period of 5–40 min, depending on the Ca<sup>2+</sup> concentration.

(5) Compare: Wagenaar, A.; Rupert, L. A. M.; Engberts, J. B. F. N.; Hoekstra, D. *J. Org. Chem.* **1989**, *54*, 2638. Similar results were obtained with vesicles formed from di-*n*-tetradecyl phosphate (DTP).

(6) (a) Gregoriadis, G., Ed. *Liposomes as Drug Carriers*; Wiley: London, 1988. (b) Machy, P.; Leserman, L. *Liposomes in Cell Biology and Pharmacology*; John Libbey: London, 1987.

(7) Bauman, R. A. *Synthesis* **1974**, *870*.

(8) Steck, T. L.; Kant, J. A. *Methods Enzymol.* **1974**, *31*, 172.

(9) Hoekstra, D.; Düzgünes, N. *Biochemistry* **1986**, *25*, 1321.

(10) Struck, D. K.; Hoekstra, D.; Pagano, R. E. *Biochemistry* **1981**, *20*, 4093.

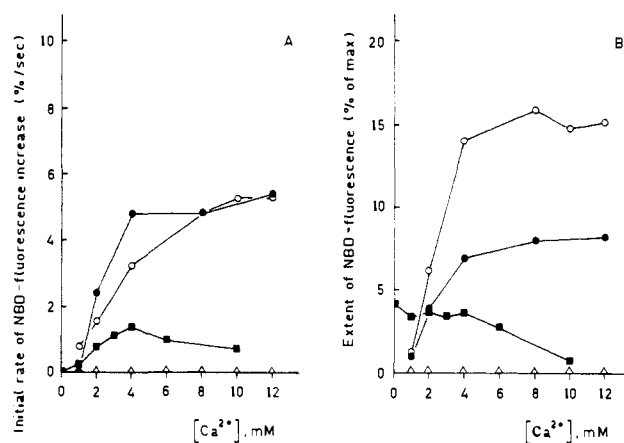
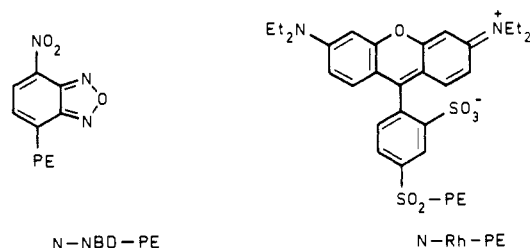


**Figure 1.** Initial rates of fusion (A) and extents of fusion (B) as a function of the Ca<sup>2+</sup> concentration for symmetric and asymmetric vesicle fusion:  $\Delta$ , DDP-PS;  $\circ$ , PS-PS;  $\bullet$ , PS-DDP;  $\blacksquare$ , DOPC-DDP. Experimental conditions: incubation temperature, 25 °C; pH 7.4; ratio of labeled to unlabeled vesicles, 1:1; total lipid concentration,  $5.0 \times 10^{-5}$  M.

**Electron Microscopy.** The occurrence of vesicle fusion was checked by transmission electron microscopy. Samples were stained with a 1% (w/v) solution of uranyl acetate after they were mounted on carbon-coated Formvar grids, which were pretreated by glow discharge in *n*-pentylamine. Micrographs were obtained with a Philips EM 300 electron microscope operating at 80 kV and with a low electron dose (<1 electron/Å<sup>2</sup>).

### Results and Discussion

Initial rates and extents of fusion for symmetric and asymmetric Ca<sup>2+</sup>-induced fusion were followed by monitoring lipid mixing with the resonance energy transfer assay.<sup>10</sup> This assay takes advantage of the efficient overlap between the emission and excitation spectrum of two nonexchangeable fluorescent phospholipid analogues *N*-(7-nitrobenz-2-oxa-1,3-diazol-4-yl)phosphatidylethanolamine (*N*-NBD-PE; donor) and *N*-(lissamine Rhodamine



*B* sulfonyl)phosphatidylethanolamine (*N*-Rh-PE; acceptor). These fluorophores can be incorporated into vesicle bilayers at concentrations that do not perturb the bilayer structure, while the efficiency of energy transfer is proportionally related to their membrane surface density. Fusion between vesicles labeled with both *N*-NBD-PE and *N*-Rh-PE and unlabeled vesicles reduces the surface density of the fluorophores, leading to a decrease of the resonance energy transfer efficiency. The concomitant increase of *N*-NBD-PE fluorescence then allows an accurate monitoring of both the rate and final extent of the fusion process. To determine whether *asymmetric* fusion could occur between vesicles formed from synthetic amphiphiles (DDP) and phospholipid vesicles, the latter were labeled with *N*-NBD-PE and *N*-Rh-PE. After mixing and addition of Ca<sup>2+</sup>, asymmetric fusion should result in probe dilution and a concomitant increase in fluorescence. Symmetric fusion will go unnoticed since the surface density of the probes remains unaltered. We find that asymmetric fusion indeed occurs readily.

Figure 1 shows initial rates and extents of fusion for asymmetric Ca<sup>2+</sup>-induced PS-DDP and DOPC-DDP vesicle systems at 25 °C and pH 7.4. Data for symmetric PS-PS vesicle fusion (mixing of labeled with unlabeled PS vesicles) are included for comparison. In the asymmetric fusion experiments, the employed temperature excludes symmetric DDP vesicle fusion, which only occurs above

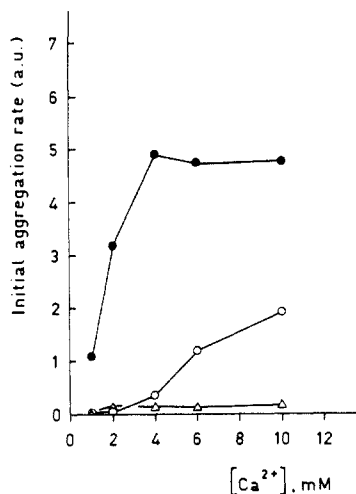


**Figure 2.** Initial rates of aggregation as a function of the  $\text{Ca}^{2+}$  concentration at 25 °C for symmetric and asymmetric aggregation of equimolar amounts of DDP and PS vesicles;  $\Delta$ , DDP-DDP;  $\circ$ , PS-PS;  $\bullet$ , PS-DDP.

the main phase-transition temperature of the DDP bilayer ( $T_m = 29$  °C).<sup>4d,11</sup> Large unilamellar DOPC vesicles ( $T_m = -22$  °C) do not undergo symmetric fusion,<sup>12</sup> whereas in the PS-DDP fusion experiments the PS vesicles ( $T_m = 7$  °C) were labeled with the nonexchangeable fluorophores, which implies that dilution of the fluorescent probes in the RET assay should be ascribed to asymmetric fusion. Interestingly, DOPC-DDP vesicle fusion also occurs spontaneously (Figure 1) albeit at a low rate. This contrasts with PS-DDP fusion, which reveals a definite  $\text{Ca}^{2+}$  threshold concentration of 1 mM comparable to the value found for symmetric PS-PS fusion. Presumably, this distinction can be attributed to differences in electrostatic repulsion, DOPC being a zwitterionic phospholipid, whereas PS is negatively charged. Furthermore, the data in Figure 1 indicate that initial rates for PS-DDP and PS-PS fusion are similar. This observation could suggest that the similarity in fusion rates was dictated by a similarity in the rates of  $\text{Ca}^{2+}$ -induced aggregation. However, separate experiments in which aggregation rates were monitored by turbidity measurements, at conditions otherwise identical with the fusion experiments, revealed that the initial rates for PS-DDP aggregation are much higher than for PS-PS aggregation (Figure 2). This implies that, in the overall fusion process, the actual membrane merging rather than membrane aggregation represents the rate-determining step. Previously, a similar conclusion was drawn for the symmetric fusion of cationic and anionic synthetic surfactant vesicles.<sup>4</sup> Most interesting is the observation that *asymmetric* PS-DDP and DOPC-DDP fusion does occur *below*  $T_m$  of the DDP vesicles. These results indicate that the target membrane for asymmetric phospholipid vesicle fusion should not necessarily reside in its liquid-crystalline state for efficient fusion to occur.

Perhaps the most striking finding in the present study is the facile  $\text{Ca}^{2+}$ -induced asymmetric fusion of DDP vesicles with human erythrocyte (ghost) membranes. The latter cell membrane system has enjoyed great popularity in recent years, and its molecular organization<sup>13</sup> and fusogenic activity<sup>14</sup> have been examined in some detail. Initial rates and extents of  $\text{Ca}^{2+}$ -induced fusion of DDP and PS vesicles with erythrocyte ghost membranes (pH

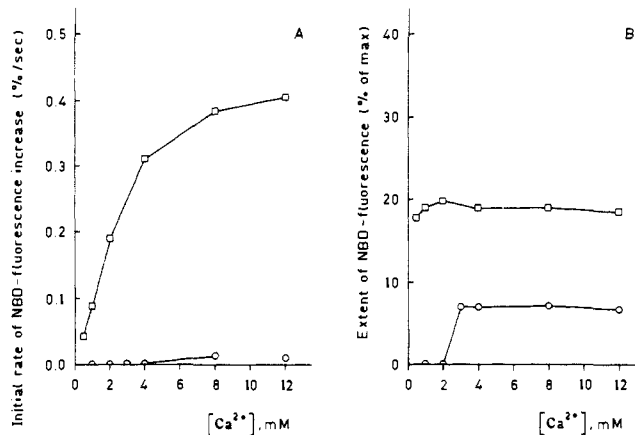


**Figure 3.** Initial rates of fusion (A) and extents of fusion (B) of DDP and PS vesicles with erythrocyte ghost membranes as a function of the  $\text{Ca}^{2+}$  concentration;  $\circ$ , PS-EG;  $\square$ , DDP-EG. Experimental conditions: see legend to Figure 1; [DDP] =  $2.5 \times 10^{-5}$  M; [EG] = 10  $\mu\text{g}$  of protein  $\text{mL}^{-1}$ .

7.4; 25 °C) are shown in Figure 3. Symmetric EG-EG fusion does not occur since this process requires phosphate anions<sup>14a,b</sup> in addition to  $\text{Ca}^{2+}$ . Although the initial rates and extents of EG-DDP fusion may slightly vary depending on the experimental conditions of ghost preparation and the origin of the blood used in the experiments, efficient lipid mixing is observed. In fact, the synthetic surfactant vesicles fuse much more rapidly and efficiently with the biological membrane than do the phospholipid PS vesicles. The reason for this result may well be that at 25 °C DDP vesicles will be solely involved in asymmetric fusion with EG membranes while, at the same conditions, PS vesicles will be engaged in massive symmetric fusion as well. The large, fused, and aggregated PS vesicles will associate to the cell surface but have largely lost the propensity to fuse.<sup>10</sup> Above  $T_m$  of DDP vesicles (e.g., >29 °C) the initial rate of asymmetric fusion with EG membranes further increases (ca. 2–3-fold at 37 °C). However, the final extent of fusion at 37 °C is only ca. 15% higher than at 25 °C. Obviously above  $T_m$ , the DDP vesicles also participate in symmetric fusion, thereby diminishing productive asymmetric fusion.<sup>15</sup>

### Conclusion

We have demonstrated that simple, synthetic di-*n*-alkyl phosphate vesicles participate in efficient fusion with both anionic (PS) and zwitterionic (DOPC) liposomes and with erythrocyte ghost membranes. An exclusively asymmetric fusion process occurs below the main phase-transition temperature of the DDP vesicles. The finding that asymmetric DDP-ghost fusion occurs faster and to a higher extent than fusion between PS and ghosts may open new avenues in attempts to devise tailored vesicular systems for use in cell biological, drug-targeting, and DNA-transfection<sup>16</sup> experiments. Further work along these lines is currently in progress.

**Acknowledgment.** The investigations were supported by The Netherlands Foundation for Chemical Research (SON) with financial aid from The Netherlands Foundation for Scientific Research (NWO).

**Registry No.** DDP, 7057-92-3; DOPC, 4235-95-4;  $\text{Ca}^{2+}$ , 7440-70-2.

(11) For DDP vesicles the cross-fusion reactions were also revealed by the observation that after fusion there was only a small tendency for a transition to a hexagonal  $\text{H}_{II}$  phase. Previously we found<sup>4c</sup> that, in the case of DDP-DDP fusion, this phase transition takes place with a high efficiency.

(12) (a) Düzgünes, N.; Nir, S.; Wilschut, J.; Bentz, J.; Newton, J.; Portis, A.; Papahadjopoulos, D. *J. Membr. Biol.* **1981**, *59*, 115. (b) Düzgünes, N.; Wilschut, J.; Fraley, R.; Papahadjopoulos, D. *Biochim. Biophys. Acta* **1981**, *642*, 182. (c) Bentz, J.; Düzgünes, N. *Biochemistry* **1985**, *24*, 54.

(13) Marchesi, V. T.; Furthmayr, H.; Tomita, M. *Annu.-Rev. Biochem.* **1976**, *45*, 667.

(14) See, for example: (a) Cullis, P. R.; Hope, M. J. *Nature* **1978**, *271*, 672. (b) Hoekstra, D.; Wilschut, J.; Scherphof, G. *Biochim. Biophys. Acta* **1983**, *732*, 327. (c) Hoekstra, D.; Wilschut, J.; Scherphof, G. *Eur. J. Biochem.* **1985**, *146*, 131. (d) Hoekstra, D.; Klappe, K.; De Boer, T.; Wilschut, J. *Biochemistry* **1985**, *24*, 4739.

(15) In addition, the formation of hexagonal  $\text{H}_{II}$  phases<sup>4</sup> effectively inhibits membrane fusion. See: Ellens, H.; Bentz, J.; Szoka, F. C. *Biochemistry* **1986**, *25*, 4141.

(16) Felgner, P. L.; Gadek, T. R.; Holm, M.; Roman, R.; Chan, H. W.; Wenz, M.; Northrop, J. P.; Ringold, G. M.; Danielsen, M. *Proc. Natl. Acad. Sci. U.S.A.* **1987**, *84*, 7413.